Beamforming by means of 2D phased ultrasonic arrays

R. Kažys, L. Jakevičius, L. Mažeika

Kaunas University of Technology, Ultrasound Research Centre

Studentų 50, 3031 Kaunas, Lithuania

Introduction

Ultrasonic phased arrays are widely used in medicine and non-destructive testing. Recently, there are attempts to apply them in ultrasonic sensors for robotics, especially intended for a navigation of mobile robots. In order to steer the ultrasonic beam in space, two dimensional (2D) arrays should be used [1-4]. The variety of array geometries and beamforming algorithms is so big that only a computer simulation can provide a reasonable solution. The main objective of this paper was to develop a computer model and the corresponding code suitable for modelling of 2D arrays with arbitrary number and location of elements, and to apply it for analysis of peculiarities of acoustic fields radiated by the 2D phased arrays in air. It is necessary also to point out that in the most models only amplitude but not the phase relations are analysed. With advent of modern digital beam forming and spatial filtering techniques, the spatial distribution of the phase variation can provide a valuable additional information for signal processing purposes. Therefore, another goal of this paper was to develop the model enabling to calculate the spatial phase variations in the acoustic fields radiated by various arrays.

Mathematical model

Let us assume that the array elements are positioned in the plane $x0y$ and each element can be excited by a signal possessing arbitrary amplitude and phase. The latter condition enables to simulate phased arrays. The model presented in the paper is suitable for continuos harmonic signals in a far field.

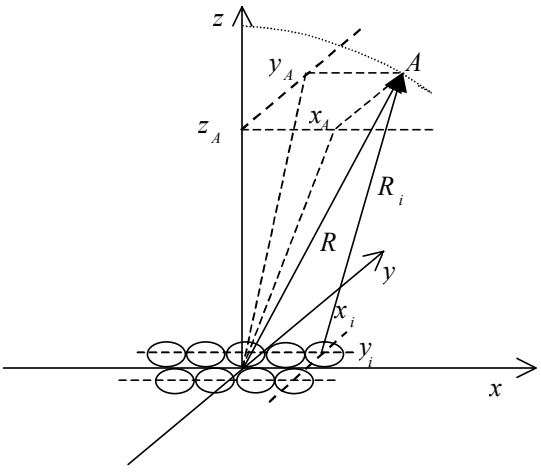

Fig.1. **Geometry of the problem**

For the sake of better graphical presentation of the calculation results a non-conventional coordinate system is used (Fig.1).

In this coordinate system the position of the point A on the spherical surface is characterised by the angles α, β, and the distance R. The angle α is between axis $0z$ and the projection of the vector R to the plane $x0z$, β is the corresponding angle in the plane $y0z$ and R is the distance between the origin of the coordinates and the point A. Then the coordinates of the point $A(\alpha, \beta, R)$ in the orthogonal coordinate system are given by

$$x_A = \frac{R\tan\alpha}{\sqrt{1+\tan^2 a+\tan^2 \beta}},$$
$$y_A = \frac{R\tan\beta}{\sqrt{1+\tan^2 a+\tan^2 \beta}}, \quad (1)$$
$$z_A = \frac{R}{\sqrt{1+\tan^2 a+\tan^2 \beta}}.$$

The distance between the i-th element of the array located at the point x_i, y_i and the point $A(\alpha, \beta, R)$ is equal

$$R_i = \sqrt{(x_A - x_i)^2 + (y_A - y_i)^2 + z_A^2}. \quad (2)$$

It has been assumed that the array consists of point-type elements, each of which however possess directivity pattern described by

$$B(\gamma) = \frac{2J_0\left(1, \pi\frac{d_e}{\lambda}\sin(\gamma)\right)}{\pi\frac{d_e}{\lambda}\sin(\gamma)}, \quad (3)$$

where $J_0(*)$ is the zero order Bessel function , d_e is the diameter of the individual element, λ is the wavelength,

$$\gamma = \arctan\sqrt{\tan^2\alpha + \tan^2\beta}.$$

The acoustic pressure produced by i-th individual element at the point $A(\alpha, \beta, R)$ is obtained combining this directivity of the element and propagation of the spherical wave:

$$p_i(\alpha,\beta,R) = B(\gamma)\frac{A_{i0}}{R_i}\cos\left[\omega t - \varphi_1(R_i) - \varphi_2(t_i)\right], \quad (4)$$

where $\frac{A_{i0}}{R_i}$ is the pressure amplitude at the distance R_i from the array element, $\varphi_1(R_i) = \omega R_i/c$ is the phase shift at the distance R_i, $\varphi_2(t_i)$ is the phase shift of the driving signal necessary for a beam deflection.

The field radiated by the whole array is obtained as a sum of the fields radiated by individual elements:

$$p(\alpha,\beta,R)=B(\gamma)\sum_{i=1}^{N}\frac{A_{i0}}{R_i}\cos\left[\omega t-\varphi_1(R_i)-\varphi_2(t_i)\right]. \quad (5)$$

The pressure amplitude can be found as

$$P(\alpha,\beta,R)=B(\gamma)\sqrt{\left\{\sum_{i=1}^{N}\frac{A_{i0}}{R_i}F_1(\varphi)\right\}^2+\left\{\sum_{i=1}^{N}\frac{A_{i0}}{R_i}F_2(\varphi)\right\}^2}, \quad (6)$$

where

$F_1(\varphi)=\sin\left[\omega t-\varphi_1(R_i)-\varphi_2(t_i)\right]$,

$F_2(\varphi)=\cos\left[\omega t-\varphi_1(R_i)-\varphi_2(t_i)\right]$

The phase of the acoustic pressure at the point $A(\square\ \square, R)$ is

$$\varphi(\alpha,\beta,R)=\arctan\frac{\sum_{i=1}^{N}\frac{A_{i0}}{R_i}F_1(\varphi)}{\sum_{i=1}^{N}\frac{A_{i0}}{R_i}F_2(\varphi)}. \quad (7)$$

The results of calculations are normalised with respect to the field value created by at the point $A(0,0,R)$ by a single virtual element located at the origin of the coordinates. In this case for the non-deflected beam $\varphi_2(t_i)=0$, $B(0)=1$, $\cos\left[\omega t-\varphi_1(R_i)-\varphi_2(t_i)\right]=1$. Therefore,

$$p(0,0,R,t)=P(0,0,R)=\sum_{i=1}^{N}\frac{A_{i0}}{R_i}. \quad (8)$$

The normalised amplitude of the acoustic field at the point $A(\square\ \square, R)$ is given by

$$P_n(\alpha,\beta,R)=\frac{B(\gamma)}{\sum_{i=1}^{N}\frac{A_{i0}}{R_i}}\sqrt{\left\{\sum_{i=1}^{N}\frac{A_{i0}}{R_i}F_1(\varphi)\right\}^2+\left\{\sum_{i=1}^{N}\frac{A_{i0}}{R_i}F_1(\varphi)\right\}^2} \quad (9)$$

The phase difference between the acoustic wave radiated by a single virtual element and the array is given by

$$\varphi_n(\alpha,\beta,R)=\arctan\frac{\sum_{i=1}^{N}\frac{A_{i0}}{R_i}\sin\left[\varphi_v(R)-\varphi_1(R_i)-\varphi_2(t_i)\right]}{\sum_{i=1}^{N}\frac{A_{i0}}{R_i}\cos\left[\varphi_v(R)-\varphi_1(R_i)-\varphi_2(t_i)\right]}, \quad (10)$$

where $\varphi_v(R)=\omega R/c$.

The validity of the model developed has been checked by comparing the directivity patterns calculated with the patterns of the linear arrays obtained by well established methods and also comparing the 2D directivity pattern of the honeycomb array with the experimental results. In both cases a good correspondance between different models and experiments was observed.

Simulation results

The main objective of the simulations was to investigate the acoustic fields radiated by different types of 2D phased arrays and find out most efficient array geometries suitable for a formation of particular fields.

Two main types of arrays were simulated;

- 2D symmetrical rectangular arrays (Fig.2a);
- 2D densely packed honeycomb arrays (Fig.2b).

Both arrays are equidistant, that is, the distance between two adjacent elements was the same and equal *d*.

The number of elements in 2D arrays can be quite big, therefore the cost of array becomes a very essential issue. Application for this purpose of low-cost ultrasonic transducers, used in commercial alarm systems, offers an efficient solution. However, the main drawback of such transducers is relatively big lateral dimensions, which can exceed the half wavelength of ultrasonic waves in air. For example, the lateral dimensions of the MURATA type 40 kHz piezoelectric transducers slightly are bigger than the wavelength. That results in a high level of sidelobes of a directivity pattern, especially at big deflection angles of an ultrasonic beam.

Therefore, we have calculated and compared the acoustic fields radiated by a few basic geometries, in which the spacing between the centres of the individual elements was equal (an ideal array) and bigger than the half wavelength of ultrasonic waves in air. The modelling was performed for the arrays operating in air at the frequency 40 kHz. The dimensions of the individual elements for all cases except the case of the ideal array correspond to the dimensions of the MURATA type transducers- the diameter of the radiating surface 9mm, the distance between the centres of the array elements 11mm. The simulation results of the arrays consisting of the 4x4 elements are presented in Fig. 3, 4, 5 and 6. In all cases the deflection angle in the *x*0*z* plane is 20°.

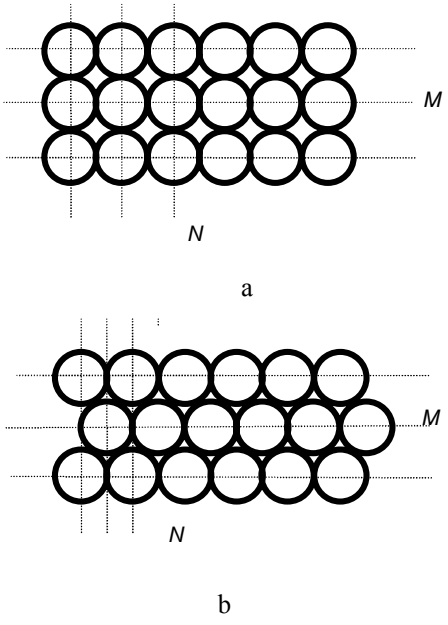

Fig.2. **Rectangular and honeycomb type arrays**

When the distance between the centres of the adjacent elements is □/2, the conventional as well as the honeycomb array possess only one main lobe in spite of the value of the lobe deflection angle (Fig. 3, 4). The arrays consisting of the MURATA type piezoelectric elements exhibit significant sidelobes, the level of which increases noticeably at bigger beam deflection angles (Fig. 5). Especially it is clearly expressed in the case of the conventional rectangular arrays. The amplitude of the sidelobes situated on the *x*-axis becomes close that of the main lobe at the deflection angle 20°. The honeycomb arrays at the same deflection angles possess significantly lower sidelobes (Fig. 6). In the vertical *x*0*z* plane practically there are no sidelobes at all, however they arise along the diagonal directed at 30° with respect to the *x*-axis. The analysis of the phase variations reveals that the phase undergoes 180° shift along the directions at which the directivity pattern has minimal values (Fig. 7).

It means, that by selecting the number and location of the individual elements in the array it is possible to achieve that the phases of the main and secondary lobes would be opposite. This can be exploited as a complementary information for post-processing of the signals transmitted by phased arrays.

Conclusions

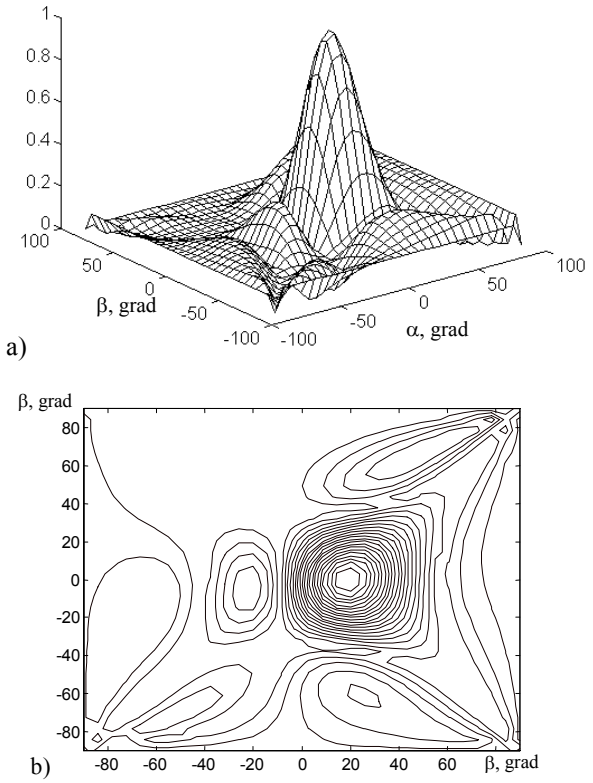

Fig.4. **Directivity patterns of the *N*=4, *M*=4 honeycomb array with the spacing between centers of the elements □ □.**

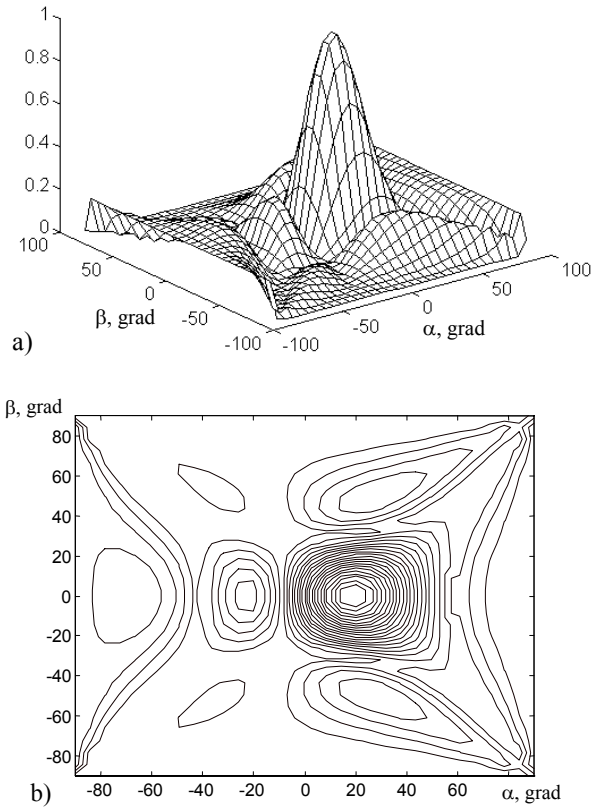

Fig.3**. Directivity patterns of the *N*=4, *M*=4 rectangular array with the spacing between centers of the elements λ/2.**

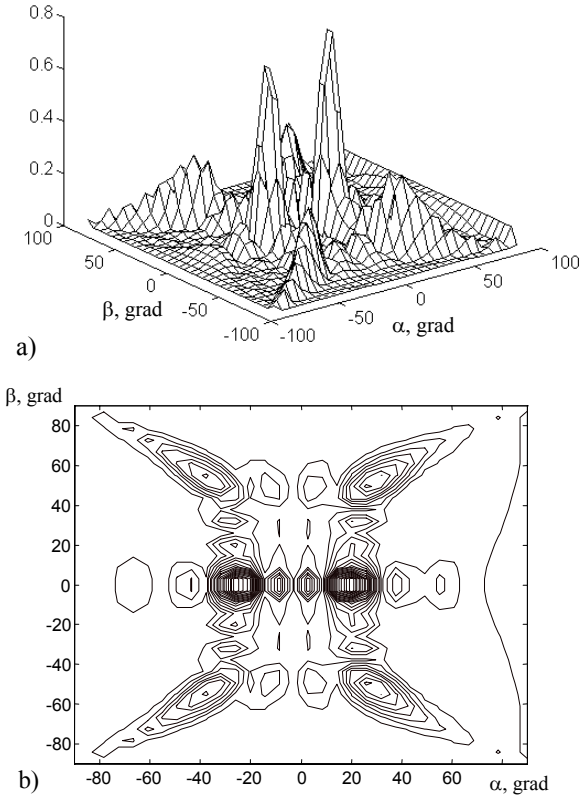

Fig.5. **Directivity patterns of the *N*=4, *M*=4 rectangular array with the spacing between centers of the elements ıı mm (d_e >λ/2).**

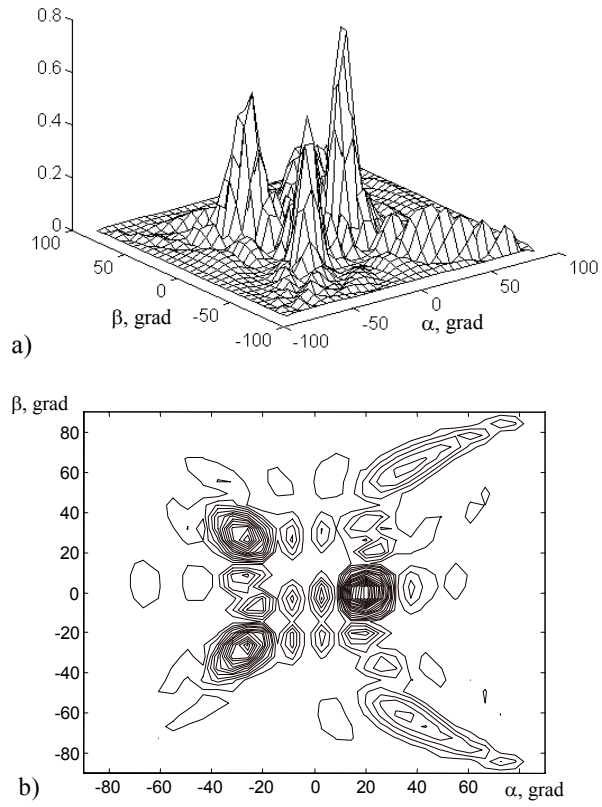

Fig.6. **Directivity patterns of the *N*=4, *M*=4 honeycomb array with the spacing between centers of the elements ı mm (d_e >λ/2).**

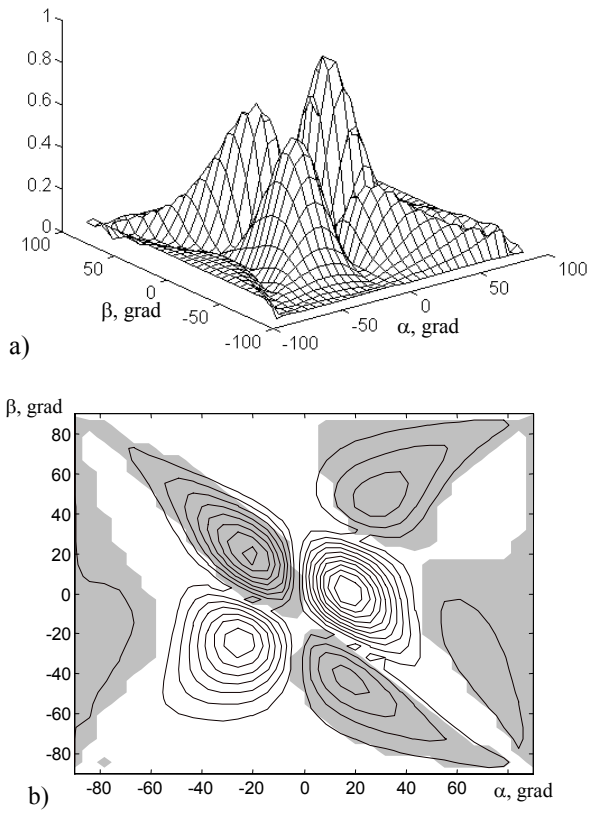

Fig.7. **Directivity pattern (a) and the spatial phase variations (b) of the *N*=2, *M*=2 honeyconb array with the spacing between centers of the elements ı mm (d_e >λ/2).**

The computer model for calculation of 2D acoustic fields radiated by 2D phased arrays with arbitrary number and location of elements has been developed. The comparison of the model developed with the other models and experimental results indicate a good correspondence. The acoustic fields presented indicate possibility to control efficiently the character of the fields radiated.

Acknowledgments

This project is sponsored by the European Inco-Copernicus programme and the Lithuanian National Science and Studies Foundation.

References

1. **W.S.H. Munro, C. Wykes**. Arrays for airborne 100 kHz ultrasound// Ultrasonics.-1994.- Vol. 32. No.1.-P.57 -64.
2. **P. Webb, C. Wykes**. High resolution beam forming for ultrasonic arrays// IEEE Trans. on Robotics and Automation.- 1996.-Vol.12. No.1.- P.138-146.
3. **G.R. Lockwood, P.C. Li, M. O'Donnell, F.S. Foster**. Optimizing the radiation pattern of sparse periodic linear arrays// IEEE Trans. on Ultrasonics, Ferroelectrics and Frequency Control.-1996.- Vol. 43. No.1.-P.7-14.
4. **G.R. Lockwood, F.S. Foster**. Optimizing the radiation pattern of sparse periodic two-dimensional arrays// IEEE Trans. on Ultrasonics, Ferroelectrics and Frequency Control.-1996.- Vol.43. No.1.-P.15-19.

R. Kažys, L. Jakevičius, L. Mažeika

Ultragarso signalų formavimas ore fazuotomis anteninėmis gardelėmis

Reziumė

Pateikti algoritmai dvimačių fazuotų anteninių gardelių su laisvai išdėstytais elementais akustinio lauko kryptingumo diagramai ir faziniam pasiskirstymui apskaičiuoti. Modeliavimo rezultatai, gauti taikant naujuosius algoritmus, buvo artimi eksperimentinių tyrimų rezultatams ir sutapo su modeliavimo rezultatais, gautais naudojant žinomus algoritmus. Tirtos galimybės sumažinti akustinių anteninių fazuotų gardelių, kurias sudarančių elementų matmenys didesni už pusę bangos ilgio, šalutinių lapelių įtaką matavimo rezultatams.

Parodyta, kad sutankintų periodinių gardelių šalutiniai lapeliai, esant faziniam kryptingumo diagramos pasukimui, išauga mažiau negu paprastos periodinės gardelės esant tam pačiam pasukimo kampui. Be to, srityse, kuriose akustinio slėgio amplitudė įgyja minimalią reikšmę, signalo fazė šuoliškai pasikeičia 180^o. Tai leidžia parinkti gardelės elementų skaičių ir išdėstymą taip, kad maksimaliai išaugusių šalutinių lapelių fazė pagrindinio lapelio atžvilgiu būtų priešinga.